The Asymmetric Schiff Bases of Streptomycin and Aniline: Coordination Chemistry, Antibacterial Screening, and In Silica ADME Study

Nagamani Lakshman, PHANIKUMARI GINKALA,PRIYANKA PAPPALA

Assistant professor,
Department of BS&H,
Visakha Institute of Engineering & Technology,
Division,GVMC,Narava, Visakhapatham, Andhra Pradesh.

ABSTRACT

The unsymmetrical Schi base ligand StmAn was used to create two new metal complexes, Ni (StmAn)2(4) and Cu (StmAn)2(5) (3). We made the ligand by reacting streptomycin (2) with aniline (1). Sub-micron elemental analysis, conductivity tests, and spectroscopic methods like 1 Methods such as hydrogen nuclear magnetic resonance (NMR), Fourier transform infrared spectroscopy (FT-IR), electron spray ionisation mass spectrometry analysis of spectra for absorption. Streptomycin's azomethine nitrogen and the N-atom of the N-methyl-L-glucosamine unit were shown to coordinate metal ions in the research. The octahedral shape was confirmed by the examination of electronic absorption spectra. complex number 4, and the tetrahedral geometry of complex number 5. Scherrer's algorithm for calculating particle size revealed their nanocrystalline nature; the complexes' shape optimization was accomplished using a Gaussian-supported MM2 task. Download the latest versions of Cs-ChemOice ultra-12.0.1 and ArgusLab 4.0.1.

Introduction

The lack of effective vaccinations and medications to treat new infectious illnesses is a problem for the whole world. The continuous COVID-19 epidemic has wreaked havoc on human society in many ways, including but not limited to the following: the economic and social climate of nations, and people's perspectives on alter one's behaviour to fit in with the surroundings [1]. A state of fear has set in. to recover from this illness as a whole. Many Drug companies supposedly found vaccinations to combat the present pandemic and also received some funding for research into potential future vaccines. success. Pathogenic organisms undergo functional

changes in biology as a result of genetic mutation. different behaviour [2]. Now more than ever, repression is difficult. their behaviour; scientists, on the other hand, are attempting to Find more effective means of limiting their effects [3, 4]. For the purpose of saving lives during pandemics, pharmaceutical companies actively pursue medication research initiatives. A antimicrobial resistance is another challenge facing medical research. antibiotic overuse and the ensuing catastrophe. Most antibiotics the medications in the drug archive have been subjected to antimicrobial drug resistance, and there are presently no new medicines in development to discovery of antibiotics in 1930 was a major step in preventing the spread of such illnesses [5, 7]. is one of the greatest contributions to health care ever made. As the third Between the second and fourth halves of the twentieth century, antibiotics were on the Excellent, particularly in the field of post-World War II injury care The state of antibiotic development and research have plateaued in terms of innovation as the pharmaceutical sector a new kind of antibiotic [10] has not been introduced. the majority of Recent antibiotics were discovered between the 1940s and the 1960s. At Around that time, the process of treating sickness relied on antibiotics, and its usage is not contested at the present time [11].Antibiotics, which were formerly only a useful tool in medicine, are now widely regarded as miracle treatments since they are the most effective chemotherapy drugs in medical history [12]. The *e Present Research on antibiotics has been seen as particularly difficult. increased interest in the subject of pharmacology, which is a fascinating drug-resistant infections pose a danger and have spawned a need for new ways of thinking and planning to reshape it [13]. Antibiotic misuse, overuse, and over prescribing in Medication resistance is mostly due to problems encountered in practical practise [14].

Experimental Section

Supplies, Number Two. The chemicals employed were all commercially available analytical reagent (AR) grade. The ligand 3 was prepared from high-purity aniline (Merck) and streptomycin sulphate (Alfa Aesar). purchased from stores and cleaned up by the normative methods now used. The copper salts used were CuCl2.2H2O and NiCl2.6H2O (Merck). Methanol (Qualifier) that has been distilled was used. chemical synthesis solvent *e bacterial culture was cultured on agar plates using the Muller

Hinton method (Himedia co.). High-quality borosilicate glass was utilised in all laboratory vessels, which were then cleaned using a three-step method. alcohol breath test before doing any scientific study.

The OMEGA melting point equipment was used to record the melting point, and the Elemental Vario EL III Germany type analyzer was used to conduct the elemental microanalysis and pH measurement. measurements were taken using a pH metre (Elico-16) and FT-IR spectra were captured using On KBr discs at room temperature using a Perkin Elmer 783 FT-IR Spectrometer within the 4000 - 4000 cm -1 range Spectra of electronic absorption microprocessor UV/Vis single-beam recorder. An Indian LT-290 spectrophotometer employed DMSO as the detection solvent. solvent between 200 and 800 nm in wavelength. 1 The 1H nuclear magnetic resonance spectrum the ligand in DMSO-d6 using TMS as an internal standard on a Bruker AV300/1 FT-NMR spectrometer reference.

Synthesis of Compounds

2.3.1 StmAn (3) Synthesis (C27H44N8O11). 2 mmol (0.2 ml) of ligand precursor (1) was added to a solution of Stm (2) (2 mmol, 1.359 g) in 30 ml hot aqueous methanol, and the pH was raised to a slightly alkaline value. pH 8 is achieved by gradually adding 2N NaOH solution to the mixture. was put on hold for 3 hours, during which time the volume of When the pink solid was added, the solution volume was cut in half. StmAn's separating product (3) was isolated by a sluggish diffusion process. purification method (recrystallization from hot methanol), and

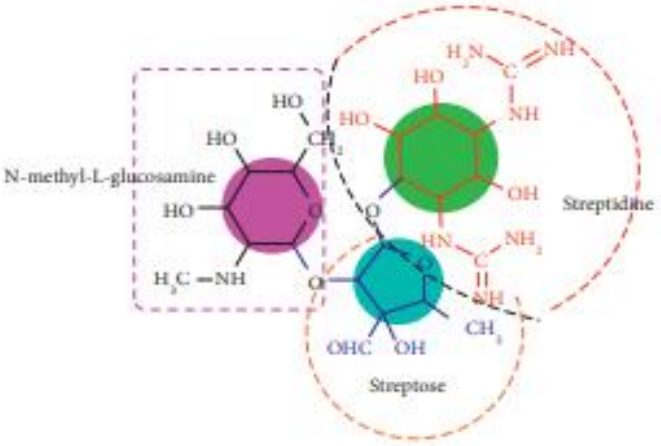

Figure 1: Structure of streptomycin.

desiccated in a vacuum dryer Scheme 1 depicts the synthetic method used to produce ligand (3) and complexes (4) and (5). The chemical formula for caffeine is C27H44N8O11. There was an 80% yield and a melting point of 187 degrees Celsius. For example, the ESI [M]+ 656.69 m/z mass

spectrum. Analytics and Calculus of Elements. C, 49.38; H, 6.75; N, 17.06; O, 26.80; Found: C, 49.53; H, 6.75; N, 17.06; O, 26.80 Spectral IR (in KBr, Angstroms, Centimeters): 6.81 for Br, 16.91 for N, and 26.95 for O : 3349.65 (b, O-H string), 1651.61 (s, C N. amine), 1113.34 (C-N string), 505.80 (NiO), 457.09 (Ni-N). Maximum wavelengths in the ultraviolet (nanometers) are 314, 340, and 347. Measured in micrometres per second, or microsiemens, the conductivity (M, S cm1) : 31.8.

Complex Synthesis, 2.3.2. StmAn (3) (2 mmol, 1.3133 gm) was dissolved in 30 ml of warm methanol, and solutions of NiCl2.6H2O (1 mmol) and CuCl2.2H2O (1 mmol) were added in increments of 10 ml. added in increments, then allowed to reflux for several hours subjected to continuous churning. The solid state colour representation of the number M (II) generated by the gradual dispersion of complexes (4) and (5) at room temperature, the solution. Filtration was performed on the solids, cleaned with alcohol, then dehydrated. In other words, [Ni (StmAn)2]. 2H2O (4). Chemistry Formula: C54H90N16NiO24. Relatively high yield (65%) and melting point (265 degrees Celsius). Spectrum of masses ESI Elements Analyzed and Calculated (Percentage): Carbon (C), 46.13; Hydrogen (H), We calculated a value of C = 46.25; H = 6.44; N = 15.87; and O = 27.31. IR (KBr,, cm1) = 27.28 the following (in base currency): 3349.65 (b, O-H str.), 1651.61 (s, 1113.34 (C-N str), 505.80 (Ni-O), 457.09 (C N. amine), and 457.09 (NiN). Maximum wavelengths for ultraviolet and visible light are (nm) 305, 317, 350, 377, 398, 698, and 763. Measured in micrometres per second, or microsiemens, the conductivity (M, S cm1) :29.8. Copper (StmAn2) (5). Molecular formula: (C)54H(86)Cu(N16)O(22). Mass spectrum ESI, melting point 278 degrees Celsius, and a 70% yield. [M]+ 1374.39 m/z. C, 47.17 (percent) in the elemental analysis calc; H, 25.60 Observed values: C = 47.15; H = 6.24; N = 16.44; O = 25.60 IR (KBr,, cm-1):3342.44 (b, O-H str.), 1654.16 (s, C-H str.) at 25.57 1113.69 (C-N str), 465.71 (C N. amine), and C N. amine (Ni-N). UV/Vis. (λmax, nm): 306, 311, 348, 377, 650. Permeability (M, S) cm−1 : 7.4.

Results and Discussion

A Description of the Body Parts 3.1. CHN analysis was used to verify molecular formulas for a Schiff base ligand and its

metal complexes. "*e CHN and others" information on the compounds' physical qualities, such as their molar The results of the synthesis are shown in terms of conductance, pH, and colour. The analytical findings show that there is a 1:2 proportion between the complexes. A ML2 psychometric and a metal-ligand molar ratio of *e molar The values for conductance spanned from 7.41 Siemen/cm to 31.8 Siemen/cm. meaning they are not electrically conductive, and they The levels are lower than one would anticipate for an electrolyte [29]. *e The arthroscopic of Complex 4 crystals suggests that Molecules of water have a role in the crystalline structure. Metal Generated ligand complexes shift conformation when colours, suggesting they resulted from chemical processes [30, 31]. Low pH levels may also be conducive to deprotonation-induced complementation with metal ions ligands. From ligand to metal, the pH of our work decreases. compounds of metals; evidence for complementation.

Spectroscopic Characterization

Experimentation using Fourier Transform Infrared (FT-IR) 3.2. Selected IR absorption peaks and spectral data of ligand 3 and its metal complexes 4 and 5 are shown in Figures S1-S3. There are a variety of e peaks in the colours of the rainbow provide important information about manufactured chemicals' chemical structure *e IR spectrum of A typical broad-band signal may be seen at 3367.45 cm-1 in Figure 3. what this means

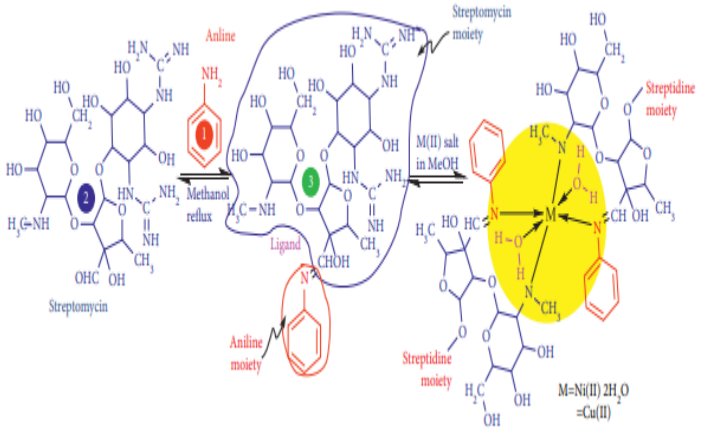

Scheme 1: Synthetic route for the preparation of ligand and metal complexes.

ascribed to] the (O-H) gap. A significant intensity band at 1663 due to the stretching of azomethine (C N). Lowered wavenumbers of 1651.61 and 1654 cm1 now characterise ligand 3. 16 cm−1 for 4 and 5, their respective, complexes [32]. A Shift in the IR Spectrum positions denotes the degree of coordination between the nitrogen atoms in the azomethine and the metal atoms. A tense rim all the way The reason why all of these chemicals have a characteristic wavelength of 1100 cm1 is

because of the (C-N) lengthen the N-methyl group at the N-methyl-L-glucosamine linkage in the streptomycin molecule [33]. Medium The metal-nitrogen connection in nitrous oxide is proven by intensity bands. signatures of metal complexes at 457.09 and 465.71 cm1 in particular, [34] *e metal-oxygen complexes 4 and 5. Complex 4 bonds are supported by a medium of hydrogen bonds. 505.80 cm1 [35] us, the infrared spectral Strong evidence for the complementation with It is plausible, according to Schiff base theory, that the ligation is caused by Nitrogen from azomethine and the nitrogen in CH3 N-methyl-L-glucosamine has a substituted amine group. subunit of Schiff bases; this information suggests that N,N donor atoms have a role in metal coordination. with relation to ligand 3.

Study 3.2.2: 1 H NMR Spectroscopy *e The 1 H NMR spectrum of ligand 3 figure S4; a summary of the spectrum data is provided in Table 1: The number of proton kinds matches up with the integral intensities of each signal in the spectrum. here and now. *e 1 A signal in H NMR at 2.5 ppm may be attributed to The proton content of the DMSO solvent. *e signal at 1.21 ppm is proposed An azomethine proton shows as a singlet at, which is determined to be the peak for CH3 protons bonded to the tetrahydrofuran ring. 7.983 ppm [36]. In pairs, the four aromatic protons The presence of doublets is seen between 6.95 and 7.4 ppm. Other protons in the ring structures of tetrahydrofuran and tetrahydropyran showing peaks between 3.798 and 4.983 ppm. *e peak in the 2.67-2.71 ppm range may be attributed to N-CH3. neutral atomic nuclei (37), also called protons. Every one of these findings agrees rather well with The ligand's suggested molecular formula.

Table 1: 1 H NMR spectral data of StmAn ligand (3)

Compounds	Chemical shift δ ppm	Assignment
	6.956–7.4	M, aromatic protons
	7.983	S, 1H, azomethine protons
	6.547	Tetrahydrofuran CH near to C-O linkage
	6.3–6.319	Tetrahydropyran CH near to C-O bond
StmAn (3)	3.798–4.983	Tetrahydrofuran and tetrahydropyran ring protons
	2.823–3.33	Cyclohexane protons
	3.79–3.54	Methylene proton
	2.671–2.712	N-Methyl protons
	1.194	Methyl protons

Three, four, and five were synthesised, and their electronic absorption spectra in DMSO were examined between 250 and 800 nm at ambient temperature. unbound ligand's spectrum comparison to room temperature [38, *e] Those metal complexes, which demonstrated the bands' durability

throughout time, showing that the ligand undergoes n and transitions in every possible compound. There has been a bathochromic change in the visible-light areas of the bands, though. spectrum in every building [39]. *e new bands were also *e electronic transitions detected in the spectra of metal complexes Important details may be gleaned from absorption spectra. *e absorption below 400 nm are attributable to the geometry of the metal complexes and the arrangement of the ligands. mutations in ligand orbital and ligand-metal charge transfer; visible-light emitted photons result from d-d transitions. *e The ligand's electronic absorption spectrum shows a maximum at a wavelength of 319 nm, which may be attributed to The Changes.

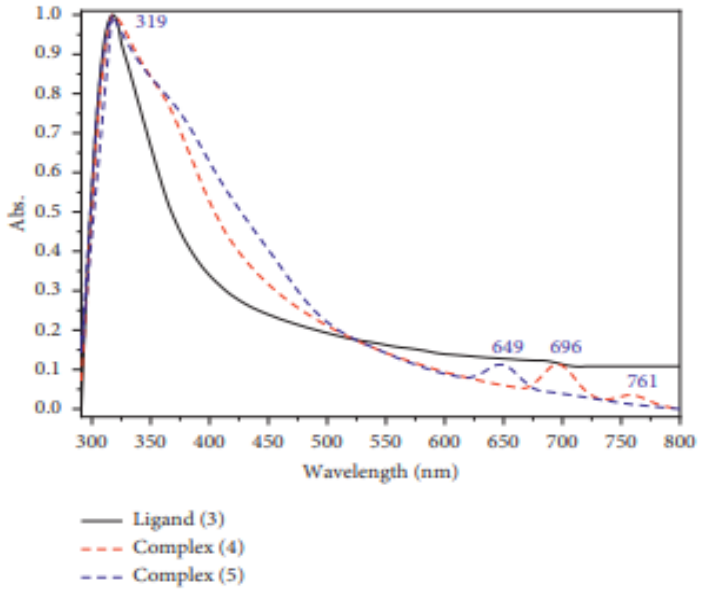

Figure 2: UV/Visible spectrum of the ligand and complexes.

The predicted molecular weight for the compounds has been determined using an ESI-Mass study, section 3.2.4. *e molecular ion peaks for the compounds have been evaluated. The molecular ion peak [M 2] was seen at m/z 656.68 amu in the positive ion ESI-mass spectra of the ligand (3). which corroborates the the ligand's suggested molecular formula a spectrum of peaks from 642.7 to 585.6 to 553.56 to 487.5 to 455.5 Assigning numbers like 412.44, 396.5, 348.5, 262.2, 242.47, etc. fragments of varying peaks Equally applicable, the ESI-mass of the positive ion Molecular ion peaks were seen in the spectra of complexes 4 and 5. corresponding to m/z 1406.13 and 1374.39 amu peak of molecular ions. To that end, the ESI-mass spectra given I Figures 3, S5, and S6 for the ligand 3

and the metal complexes 4 and 5 are supportive of the suggested structure.

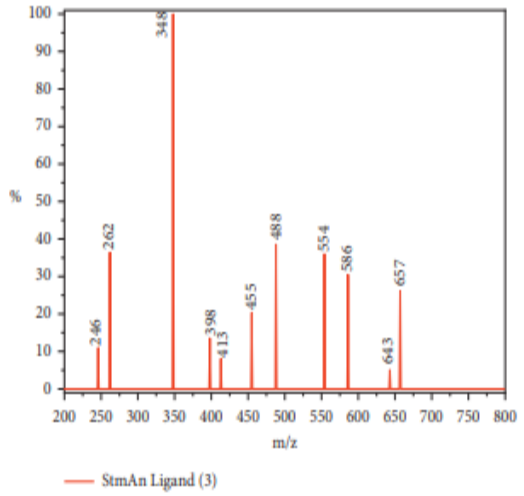

Figure 3: Mass spectrum of ligand (3)

To learn more about the crystals, we performed a powder X-ray diffraction study (PXRD) [44, 45] It was determined that the ligand and metal complexes were crystalline by observing their powder diffraction patterns (Figure 4). Solid evidence The results of analyses of structural refinement and In Table 2, we see that the ligand's average crystallite size (3) and its Scherer's formula was used to determine the metal complexes (4) and (5). where is the wavelength, is the angle between the incident and reflected rays, and dXRD = 0.9/Cos. complete breadth at half maximum of the distinctive peak, and The diffraction angle for the plane of reflection is [46, 47]. The ligand had eleven measured reflection peaks (3) interplanar distance d = 2.028A, maximum intensity = 2 44.64°. There were 12 reflection peaks for complex (4). been seen with a peak at 44.65° and a matching d spacing value of 2.03A. Exhibited 11 Complex Features, 5 of Which Were strong reflection peaks around 15.45°, where the d spacing value is 5.73A on average for crystalline materials. It was determined that the sizes of 10.81 nm, 12.72 nm, and 11.96 nm shown to be nanocrystalline are ligand (3), complexes (4) and (5).

Research Using Molecular Models, Section 3.2.6 In order to comprehend the hexa- and tetra-coordination of complexes (4) and (5), 3D molecular modelling of the suggested structure was performed.

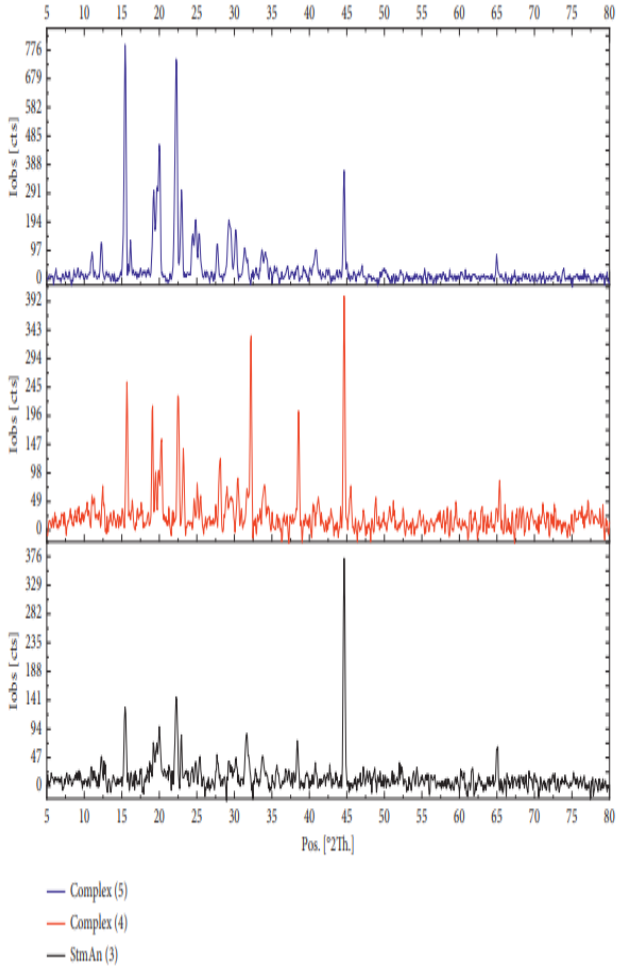

Figure 4: Powder XRD pattern of the ligand and metal complexes

using the software packages CsChemOffice 3D Ultra 12.0.1 and ArgusLab 4.0.1 version [50, 51]. Results from the investigation showed that complex (4) has an octahedral geometry, whereas complex (3) has a tetrahedral geometry (5). Altering molecular coordinates led to the establishment of the intended stereochemistry. achieve a shape of low energy and optimal molecular fit [52]*e maximum stability conformer was thoroughly tuned via molecular functions in orbits PM3 is backed by Molecular Workflows in ArgusLab computer programmes for modelling [41]. Multiple efforts were made to optimise energy use and find the optimum. Some Table 3 provides a selection of bond lengths and bond angles. optimise structures, with with atom labels, of the Figure 5(a) and 5(b) depict complexes (b). *e The bond angles surrounding the are calculated using modelling tools to Octahedral and tetrahedral structures are very well supported by metal cores. the corresponding geometries for the complexes (4) and (5). *e Complexes' minimal geometrical energy, optimized With CsChemOffice 3D Ultra and the MM2 method, coincided with those obtained using the ArgusLab package for numerical analysis. For the two last complexes (4 and 5), the geometrical energy was A value between 493.4026 and 991.4023 Kcal/mol. Also, the shift coordination is present when the bond lengths of the metal-nitrogen and metal-oxygen complexes are shorter than those of the ligands. A change was made so that (1.265A) = (1.286 A/1.281 A) and () = (1.265A). ratio of (1.270A/1.291 A) for the (4 5) and (4) complexes .

Antibacterial Activity Test (3.2.7) Recent developments in pharmaceutical research have highlighted the importance of metals as chemotherapeutic agents in drug delivery systems. Metals serve as synthetic scaffolding, however they may add features that improve vectors for delivering drugs Metals have little biological effect and can't be used to make many organic medications need to form complexes with metals in order to function properly [55, 56]. Antimicrobial properties, therefore, were investigated. ligand activity (3), ligand complexes (4), and (5). For this study, four bacterial pathogens were isolated from clinical samples. E. coli, Klebsiella pneumoniae, Proteus mirabilis, and Staphylococcus aureus identified by their ability to interact in vitro with ligand 3 chemical compounds of metals (4 and 5). Inhibition of bacterial growth was *e bactericidal effects were measured by the size of the zone of inhibition surrounding each disc (in millimetres). according to the data reported in Table 4, complexes 4 and 5 stronger than both its parent ligand and ligand 3 antibiotic chemical (Streptomycin) effective against all four bacterial disease-causing organisms. *e The relative efficacy of the the control medication Amikacin, and all of the synthetic substances

Table 2: Crystal data of ligand (3) and complexes (4) and (5).

No.	Pos. [°2θ]	FWHM [°2θ]	d-spacing (Å)	Crystallite size (nm)	Dislocation density x 10^{-3}	Microstrain × 10^{-3}	Crystallinity (%)
				Ligand (3)			
1	12.30399	0.6741	7.187889047	11.85329233	7.11741041	27.2881996	40.9695
2	15.4787	0.66053	5.720046042	12.1377064	6.787764155	21.20681317	
3	19.75461	1.47062	4.490527095	5.483276532	33.2598053	36.85273177	
4	22.29616	0.79582	3.98406262	10.17450508	9.659917424	17.62079005	
5	23.88044	3.12614	3.723216215	2.597443745	148.2203038	64.50369908	
6	29.95229	1.27797	2.980842646	6.434905725	24.1499159	20.84535886	
7	31.6725	0.66204	2.822759743	12.47312221	6.427611885	10.18383259	
8	33.85303	0.6926	2.645761149	11.98964513	6.95644478	9.930173115	
9	38.37317	0.66932	2.343862736	12.5672636	6.331674073	8.392743758	
10	44.64285	0.62174	2.028161493	13.81251239	5.241488518	6.607579026	
11	65.01222	0.48709	1.433410844	19.33953992	2.673669512	3.335316571	
			Average crystallite size	10.80574664			
				Complex (4)			
1	15.68908	0.6622	5.643814342	12.11013835	6.818703253	20.97182031	48.26636
2	19.15657	0.66244	4.62934461	12.16201431	6.760658202	17.12878329	
3	20.09317	0.80305	4.415621485	10.04669922	9.907251754	19.77793527	
4	22.60666	0.89633	3.930039146	9.038445974	12.24087511	19.56661157	
5	28.02882	0.67538	3.180876989	12.12355449	6.803620208	11.80672423	
6	29.44258	0.92938	3.031276751	8.838068674	12.80221912	15.43407942	
7	30.53251	0.49503	2.925505563	16.63510466	3.613673616	7.913851643	
8	32.12735	0.63034	2.783826403	13.11526948	5.813605569	9.551628989	
9	33.9647	0.62605	2.637317333	13.26810257	5.680445003	8.944706249	
10	38.5021	0.56194	2.336310083	14.97458933	4.459540973	7.020823841	
11	44.64861	0.62393	2.027913219	13.76431442	5.278260623	6.629904843	
12	65.28377	0.5704	1.428103966	16.53991794	3.655386462	3.885429101	
			Average crystallite size	12.71801828			

				Complex (5)			
1	15.45254	0.58949	5.729670737	13.60001133	5.406565384	18.95845355	52.7245
2	19.72787	1.02358	4.496553373	7.87773181	16.11378693	25.68568043	
3	22.29496	0.75955	3.984274344	10.66033563	8.799505029	16.81863984	
4	24.87372	1.11216	3.576741784	7.314765809	18.68956303	22.00390067	
5	27.70859	0.48612	3.216906851	16.83191598	3.529660143	8.600376122	
6	29.35107	0.71351	3.040519033	11.50958473	7.548848179	11.88777525	
7	30.20031	0.51968	2.956924934	15.83358953	3.988790581	8.403755935	
8	31.46701	0.63934	2.840723072	12.90943919	6.000469705	9.902253407	
9	33.93973	1.01346	2.639200516	8.195629902	14.88796446	14.49114036	
10	40.77191	0.74064	2.211330767	11.4429506	7.637020455	8.696173563	
11	44.64942	0.56001	2.027878311	15.33542905	4.252145704	5.95056869	
			Average crystallite size	11.956			

Figures 6-8 provide a bar chart illustrating the bacterial pathogens. The superior antibacterial activity of the synthesized compounds is shown by the antibacterial results. at their peak intensity. As an added bonus, the antimicrobial The complexes have improved ability to suppress development. After metal-ligand chelation, *eir MIC Scientific investigations showed that the ligand and complexes' antibacterial activity could be quantified with high accuracy. We're at the bottom, literally. The minimal inhibitory concentration (MIC) for ligand 3 was found as 0.0485 g/mL. A high concentration of S. aureus bacteria was found, followed by S. pneumoniae (0.097 g/L). In this study, the MIC for Complex 4 was found to be 0.024 g/L. with the bacterium S. aureus The results from complex 5 are similar. increased effectiveness against S. aureus and other germs bacterium S. pneumoniae. In conclusion, the MIC research the highest level of antibacterial activity among the synthesized chemicals with Gram-positive bacteria.

Table 3: Selected bond lengths, bond angles, and energy parameters of metal complexes.

Complex	Atoms	Bond length (Å)	Atoms	Bond angle (°)	Optimized energy (Kcal/mol)
Complex 4	O (77)-Ni (76)	1.851	O (77)-Ni (76)-O (80)	67.246	493.4026
	O (80)-Ni (76)	1.861	O (77)-Ni (76)-N (66)	159.305	Octahedral geometry
	N (66)-Ni (76)	1.332	O (77)-Ni (76)-N (37)	92.820	Stretch: 105.9509
	N (37)-Ni (76)	1.307	O (77)-Ni (76)-N (39) O (77)-Ni (76)-N (68)	84.375	Bend: 229.2888
	N (39)-Ni (76)	1.887	O (80)-Ni (76)-N (66)	82.878	Stretch-bend: 7.6676
	N (68)-Ni (76)	1.895	O (80)-Ni (76)-N (37)	92.108	Torsion: 113.0913
	C (61)-N (68)	1.286	O (80)-Ni (76)-N (39)	159.574	Non-1, 4 VDW: -38.2430
	C (32)-N (39)	1.281	O (80)-Ni (76)-N (68)	85.665	1, 4 VDW: 102.3171
			N (66)-Ni (76)-N (37)	83.089	Dipole/dipole: -26.6702
			N (66)-Ni (76)-N (39)	107.874	
			N (66)-Ni (76)-N (68)	95.903	
			N (37)-Ni (76)-N (39)	93.606	
			N (37)-Ni (76)-N (68)	88.044	
			N (39)-Ni (76)-N (68)	99.408	
			Ni (76)-N (68)-C (69)	165.518	
			Ni (76)-N (68)-C (61)	116.664	
			Ni (76)-N (66)-C (75)	114.392	
			Ni (76)-N (66)-C (59)	123.069	
			Ni (76)-N (39)-C (40)	130.059	
			Ni (76)-N (39)-C (32)	123.817	
			Ni (76)-N (37)-C (46)	120.999	
			Ni (76)-N (37)-C (30)	127.313	
				128.841	
Complex 5	N (66)-Cu (76)		N (66)-Cu (76)-N (37)	112.055	991.4023
			N (66)-Cu (76)-N (39)	114.873	Tetrahedral geometry
	N (37)-Cu (76)	1.869	N (66)-Cu (76)-N (68)	100.215	Stretch: 281.4662
		1.920	N (37)-Cu (76)-N (39)	93.120	Bend: 206.2694
	N (39)-Cu (76)	1.328	N (37)-Cu (76)-N (68)	128.136	Stretch-bend: 32.5374
		1.380	N (39)-Cu (76)-N (68)	109.129	Torsion: 123.9495
	N (68)-Cu (76)	1.291	Cu (76)-N (68)-C (69)	126.904	Non-1, 4 VDW: 218.1859
		1.270	Cu (76)-N (68)-C (61)	119.491	1, 4 VDW: 149.6583
	C (61)-N (68)		Cu (76)-N (66)-C (75)	116.111	Dipole/dipole: -20.6644
	C (32)-N (39)		Cu (76)-N (66)-C (59)	129.044	

The ADME Study in Switzerland, Version 3.2.8 One of the most rapidly expanding areas of study nowadays is medicinal chemistry. The bad news is that creating a new drug takes tens of millions of dollars and tens of years. drug [57]. In reality, estimates range from the tens of thousands

to the compounds, one substance may meet all the requirements for get regulatory approval for use as a pharmaceutical. More than half of these substances evaluation of physicochemical qualities that fail may substantially aid medication development procedures that might otherwise It is the ADMET characteristics that try to foretell the hit chemicals. (Table 6) [58].

Chemical compound destiny is linked to absorption, distribution, metabolism, excretion, and toxicity, abbreviated as ADMET. Swiss Web server ADME calculates the structure-based physicochemical properties compounds (http://www.swissadme.ch/). as a result of Large structures prevented accurate calculations of metal complexes. To that end, we may now examine the prepared Schiff base's in silica characteristics. compare it to streptomycin, which is a close relative. It's worth noting that streptomycin, the antibiotic used to treat strep throat, It has received regulatory approval as a pharmaceutical Hemispherical properties that are so interesting do not "fall inside" the acceptable criteria range described above [59], therefore If not, [58] *e molecule server on the web (https://mcule.com/), which, among other things, may be measured the compound's nonpoisonous *is molecule web displayed. server indicated the presence of a potentially hazardous substructure in the *e Schiff base and the antibiotic streptomycin are the forerunners of this compound. Tables S1 and S2 include the pharmaceutical and drug-likeness data, respectively.

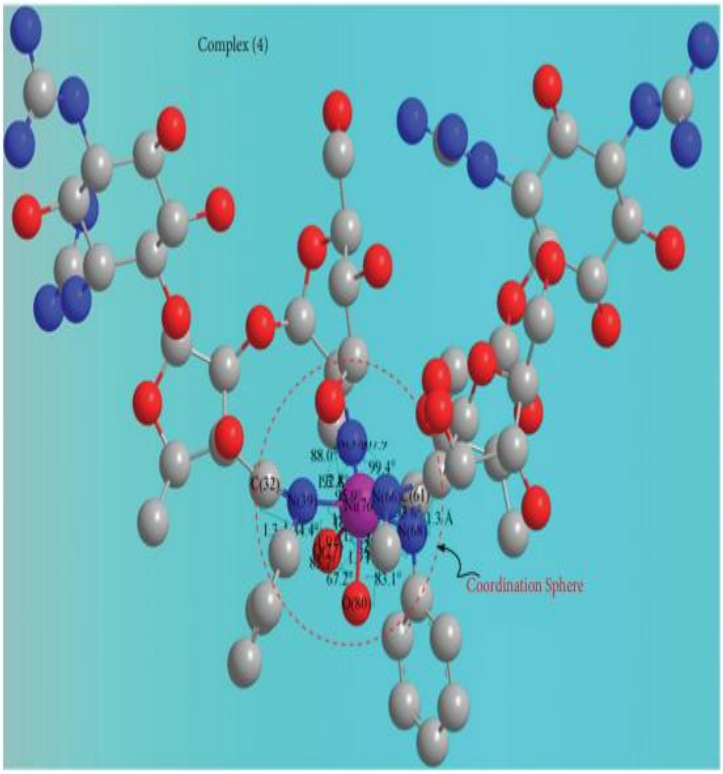

(a)

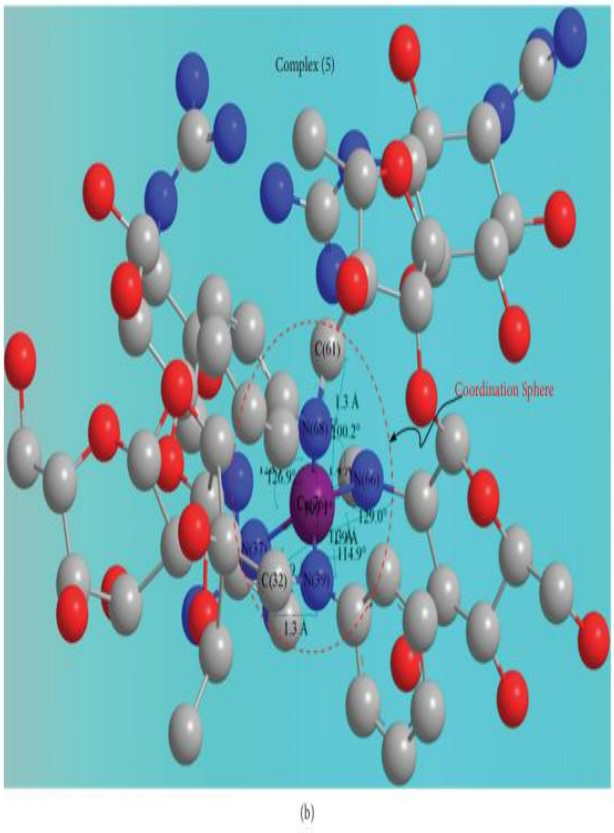

Figure 5: 3D-optimized structures of (a) complex (4) and (b) complex (5).

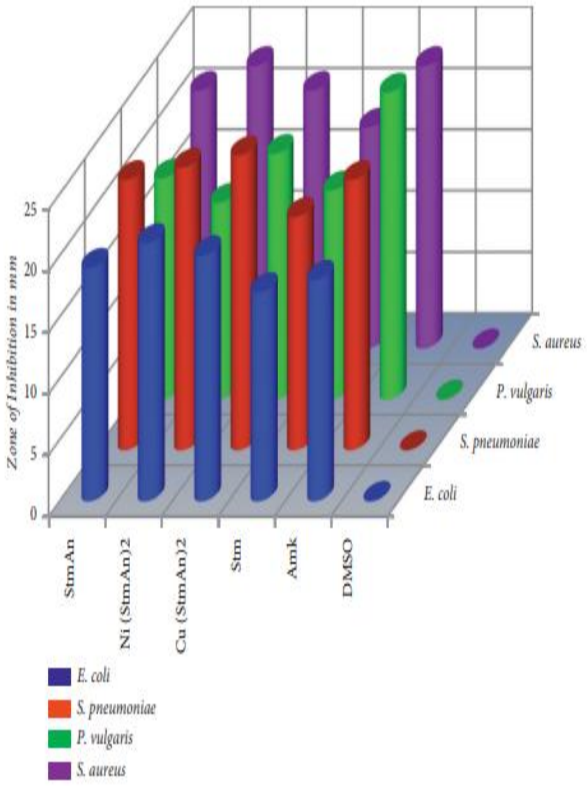

Figure 6: Bar graph showing the antibacterial activity at 100 µg/µL concentration.

Table 4: Antibacterial activity data.

Compounds	Diameter of zone of inhibition in mm											
	E. coli			*S. pneumoniae*			*P. vulgaris*			*S. aureus*		
Concentration (µg/µL)	100	50	25	100	50	25	100	50	25	100	50	25
StmAn, 3	19	15	12	22	18	15	18	14	11	21	13	11
Ni (StmAn)2, 4	21	16	10	23	19	15	16	10	9	23	17	10
Cu (StmAn)2, 5	20	15	10	24	20	13	20	15	10	21	15	12
Stm, 2	17	15	8	19	18	14	17	13	9	18	10	10
Amk	18	18	18	22	22	22	25	25	25	23	23	23
DMSO	0	0	0	0	0	0	0	0	0	0	0	0

Table 5: Minimum Inhibitory Concentration (MIC) data.

Compound	Minimum inhibitory concentration (MIC) in (µg/µL)			
	E. coli	*S. pneumoniae*	*P. vulgaris*	*S. aureus*
StmAn, **3**	0.39	0.097	0.39	0.048
Ni (StmAn)2, 4	0.097	0.048	0.19	0.024
Cu (StmAn)2, 5	0.39	0.048	0.39	0.048
Stm, 2	0.19	0.024	0.097	0.097
$NiCl_2$	na	na	na	na
$CuCl_2$	na	na	na	na

na = no activity.

Table 6: Results of hemispherical properties obtained from SwissADME web server.

Physicochemical properties[a]		
Formula	$C_{21}H_{39}N_7O_{12}$	$C_{27}H_{44}N_6O_{11}$
Molecular weight	581.57 g/mol	656.69 g/mol
Num. rotatable bonds	11	12
Num. H-bond acceptors	15	15
Num. H-bond donors	14	14
Molar refractivity	130.43	158.96
TPSA	331.43 Å^2	326.72 Å^2
Lipophilicity (Log $P_{o/w}$)	−5.87	−4.34
Water solubility	Highly soluble	Highly soluble

[a]The first column is the data of streptomycin, and the second is of Schiff base.

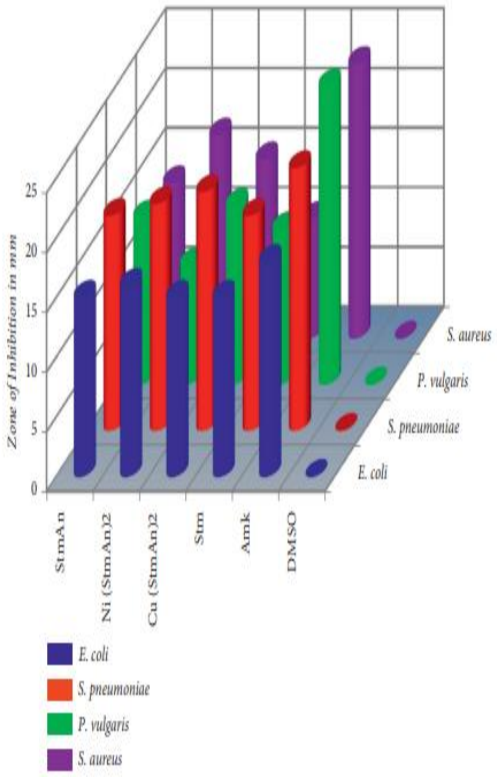

Figure 7: Bar graph showing the antibacterial activity at 50 µg/µL concentration.

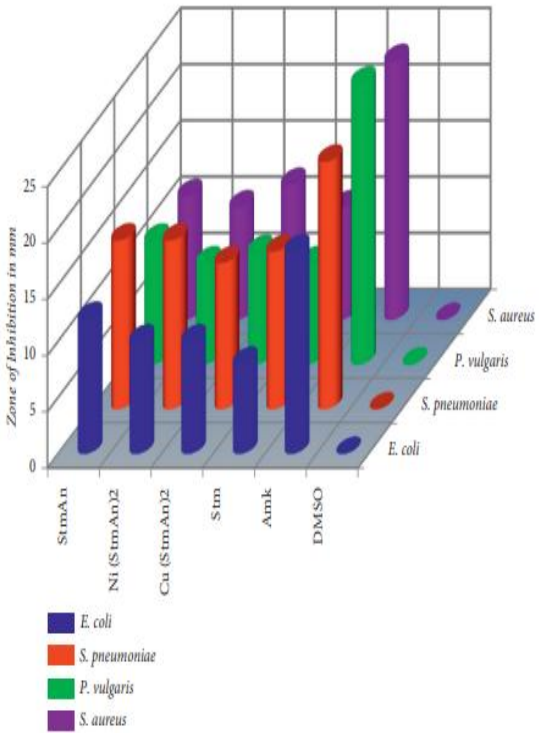

Figure 8: Bar graph showing the antibacterial activity at 25 µg/µL concentration.

Conclusion

Condensation of precursors 1 and 2 yielded hypoglycaemia Schiff base ligand (3), which was then used in the synthesis of two new metal complexes, 4 and 5. In addition to 3's polydentate character, the complexity of To form Ni(II) and Cu(II) ions, N, N donor atoms were used. This research was confirmed by several investigations using other spectrum methodologies. To all substances molecular conductance

measurements showed that the compounds being generated were not electrolytic.*e IR spectral investigation verified the ligandmetal coordination through azomethine nitrogen and Streptomycin's N-atom in its N-methyl-L-glucosamine ring fraction, as seen by a change in the distribution of complexes' spectra *e particle size determination by They were Polycrystalline, as indicated by Scherrer's formula. Combining octahedron and tetrahedral geometries for complex 4, difficult (5) geometry assignments, which were additional help from a wide range of MM2 molecular models energy savings and energy efficiency calculations antimicrobial information indicated that ligand 3 had a more potent impact in preventing growth than in comparison to the active medication ingredients (2) and the placebo medicine Amikacin. All bacterial pathogens were more susceptible to the improved antibacterial action of the *e metal complexes. SwissADME Data Both the ligand (3) and the streptomycin precursor antibiotic were found to have potentially hazardous substructures via the Molecule web server.

References

[1] I. Chakraborty and P. Maity, "COVID-19 outbreak: migration, effects on society , global environment and prevention," Science of the Total Environment, vol. 728, Article ID 138882, 2020.

[2] A. A. Dawood, "Mutated COVID-19 may foretell a great risk for mankind in the future," New Microbes and New Infections, vol. 35, Article ID 100673, 2020.

[3] Z. D. Berger, N. G. Evans, A. L. Phelan, and R. D. Silverman, "Covid-19: control measures must be equitable and inclusive," BMJ, vol. 368, Article ID m1141, 2020.

[4] G. Rohith and K. B. Devika, "Dynamics and control of COVID-19 pandemic with nonlinear incidence rates," Nonlinear Dynamics, vol. 101, no. 3, pp. 2013–2026, 2020.

[5] E. D. Brown and G. D. Wright, "Antibacterial drug discovery in the resistance era," Nature, vol. 529, no. 7586, pp. 336–343, 2016.

[6] K. Bush, "Antibacterial drug discovery in the 21st century," Clinical Microbiology and Infections, vol. 10, pp. 10–17, 2004.

[7] S. J. Projan, "Why is big Pharma getting out of antibacterial drug discovery?" Current Opinion in

Microbiology, vol. 6, no. 5, pp. 427–430, 2003.

*[8] R. Gaynes, "*e discovery of penicillin-new insights after more than 75 years of clinical use," Emerging Infectious Diseases, vol. 23, no. 5, pp. 849–853, 2017.*

[9] E. J. Rosi-Marshall and J. J. Kelly, "Antibiotic stewardship should consider environmental fate of antibiotics," Environmental Science and Technology, vol. 49, no. 9, pp. 5257-5258, 2015.

[10] R. Quinn, "Rethinking antibiotic research and development World War II and the penicillin collaborative," American Journal of Public Health, vol. 103, no. 3, pp. 426–434, 2013

